SUPPORTING INFORMATION

Gauging Colloidal and Thermal Stability in Human IgG1 – Sugar Solutions through Diffusivity Measurements

Jonathan Rubin,[1,2] Aditi Sharma,[1,2] Lars Linden,[3] Andreas S. Bommarius,[1,2,4] Sven H. Behrens[1,2]

1: School of Chemical & Biomolecular Engineering, Georgia Institute of Technology, Atlanta, Georgia 30332-0100

2: Parker H. Petit Institute of Bioengineering & Bioscience, Georgia Institute of Technology, Atlanta, Georgia 30332-0363

3: Bayer Healthcare AG, Global Biologics, Wuppertal 42096, Germany

4: School of Chemistry & Biochemistry, Georgia Institute of Technology, Atlanta, Georgia 30332-0400

Refractive Index of Sugar Solutions

Refractive index measurements were conducted at 20 °C using a digital Libby refractometer (Figure S1). The buffer alone gave a refractive index of 1.3342 (y-intercept).

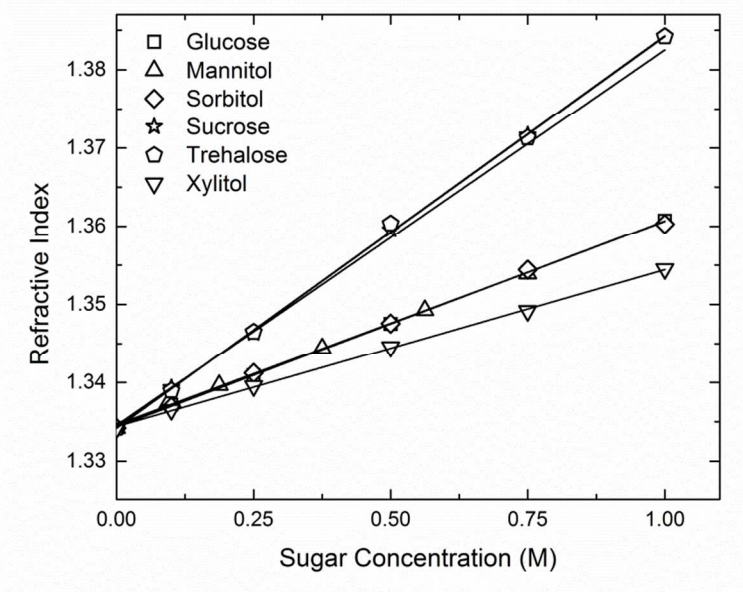

Figure S1: Refractive index measurements of a variety of sugars in buffer (25 mM acetate, 150 mM sodium chloride, pH 5.5)

Table S1: Presented are the slopes of the curves shown in Figure S1 and the refractive indices at 500 mM of each sugar. The y-intercept for all curves was 1.3342 (i.e. buffer).

Sugar	***dn/dc*** **(M^{-1})**	**RI at 500 mM**
Glucose	0.0263	1.3475
Mannitol	0.026	1.3472
Sorbitol	0.0262	1.3476
Sucrose	0.05	1.3596
Trehalose	0.05	1.3603
Xylitol	0.02	1.3446

Viscosity of Sugar Solutions

The dynamic viscosity η of buffer solutions with 500 mM sugar was determined by measuring the diffusivity D of stably dispersed 200 nm standard polystyrene (PS) particles (Bangs Laboratories Inc., Fishers, Indiana) at high particle dilution and comparing it with the diffusivity in sugar-free buffer solution. The diffusivity is inversely proportional to the medium viscosity according to the Stokes-Einstein relation

$$D = \frac{k_B T}{6\pi\eta R_h}, \qquad \text{(Equation S1)}$$

where k_BT is the thermal unit and R_h the hydrodynamic particle radius; we can therefore relate the unknown viscosity η of the sugar solution to the known buffer viscosity via

$$\eta = \frac{D_{buffer}}{D}\eta_{buffer} . \qquad \text{(Equation S2)}$$

The particle diffusivities were measured by DLS using a Malvern Zetasizer ZS90 (Worcestershire, UK). Results for the viscosities are listed below in Table S2.

Table S2: Viscosity of 500 mM sugar solutions at 25 ^{o}C

Sugar	η [mPa*s]
Buffer	0.89
Glucose	1.11
Mannitol	1.19
Sorbitol	1.11
Sucrose	1.46
Trehalose	1.58
Xylitol	1.06

Evaluation of the Interaction Parameter k_D

Figure S2 shows the apparent hydrodynamic radius $R_h(c)$, related to the actual protein diffusivity through Equation S1, and measured by DLS in glucose at 25 ^{0}C. The y-intercept of the linear regression provides the hydrodynamic radius at infinite dilution R_o.

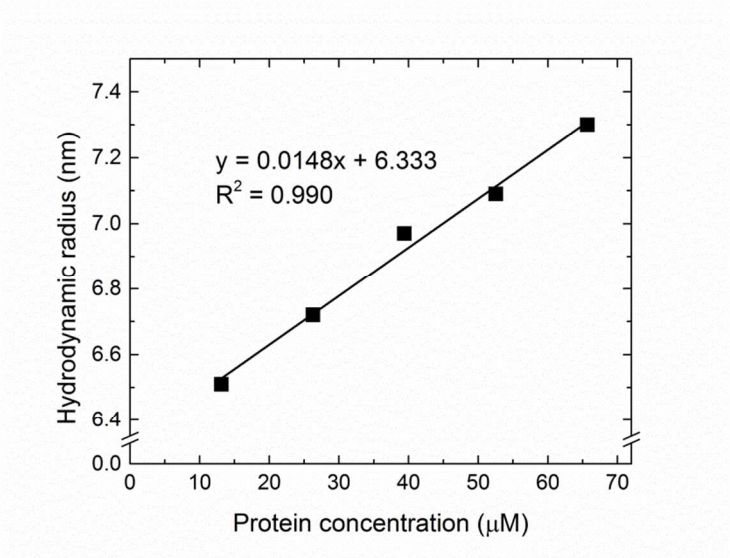

Figure S2: Apparent hydrodynamic radii versus protein concentration in buffer with 500 mM glucose

The hydrodynamic radius is related to the mutual diffusion coefficient in the Einstein-Stokes equation (Eqn. S1). Combining Einstein-Stokes with Equation 1 from the text, we can plot:

$$\frac{R_{h,0}}{R_h(c)} = \frac{D(c)}{D_0} = 1 + k_D c + O(c^2)\,. \qquad \text{(Equation S3)}$$

Figure S3 presents a graphical solution to Equation S3 for the data in Figure S2. The interaction parameter k_D is the slope of this curve (shown in Fig. S3 with units of μM^{-1}).

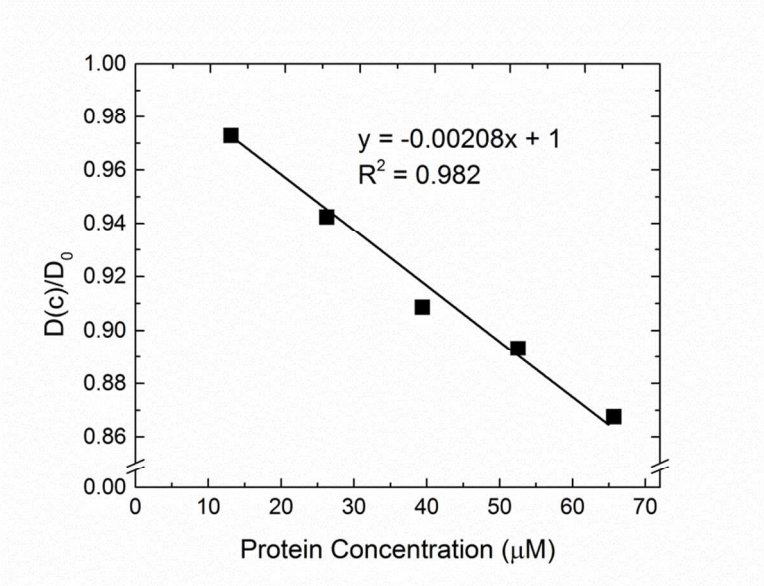

Figure S3: Normalized diffusion coefficients versus protein concentration.

Evaluation of the Initial Aggregation Rate Constant k_{11}

The rate constant k_{11} of doublet formation can be obtained with relative ease using DLS. The initial increase of the protein's hydrodynamic radius R_h at the onset of aggregation satisfies eqn. S4,[1]

$$\frac{1}{R_h(0)}\left(\frac{dR_h(0)}{dt}\right)_{t\to 0} = \frac{I_2(q)}{2I_1(q)}\left(1 - \frac{R_{h,1}}{R_{h,2}}\right)k_{11}N_1 \quad , \qquad \text{(Equation S4)}$$

where $R_h(0)$ is the initial value before aggregation sets in, $R_{h,1}$ and $R_{h,2}$ are the hydrodynamic radii of a single protein and a doublet, respectively, and I_1 and I_2 are their respective form factors. N_1 is the original number concentration of non-aggregated proteins in solution. The scattering intensities in principle depend on the scattering angle through the wave vector **q**. However, the small proteins considered in this study act as point scatterers for the 830 nm laser wavelength used ($q\,R_h << 1$); therefore, we may safely approximate $I_2/2I_1$ as unity. Using the geometric relation $R_{h,2}/R_{h,1} = 1.38$ for spheres,[1] the measured initial change in size, and rearranging eqn. S3, the equation simplifies to

$$k_{11} = \frac{0.275}{R_h(0)N_1}\left(\frac{dR_h(0)}{dt}\right)_{t\to 0} \quad . \qquad \text{(Equation S5)}$$

From eqn. S5 we can solve for the coagulation rate constant k_{11} experimentally, given that we know N_1 (the number density of monomers we begin the experiment with), by measuring $dR_h(0)/dt$ via DLS, as in Figure 2 of the article. From Figure 2 we can obtain $R_h(0)$ (y-intercept) and dR_h/dt at t = 0 (initial slope). To ensure that our evaluation of the "initial slope" truly reflects the initial stage of aggregation only, *i.e.* a time window before the average protein size is significantly impacted by higher order oligomers, we restrict our analysis to times in which the size average grows by no more than 15-20%. This is a much shorter time frame than the "coagulation half-time" of diffusion-limited aggregation, which is often used to identify the early stages of aggregation processes.[1]

Reversibility of Protein Unfolding

To investigate whether the sugar-stabilized intermediate was formed reversibly, we studied the circular dichroism upon reversing temperature ramps. From previous experiments, the temperature at which the intermediate formed was known. Figures S4 shows the CD signal during forward and reverse temperature ramp in the presence of trehalose. We wanted to determine the stability of the intermediate, so the maximum temperature was held for 15 minutes. The antibody did not melt at this temperature; rather, the signal returned to its native baseline. This result reveals that our unfolding is kinetically controlled to some extent and that formation of the intermediate is reversible.

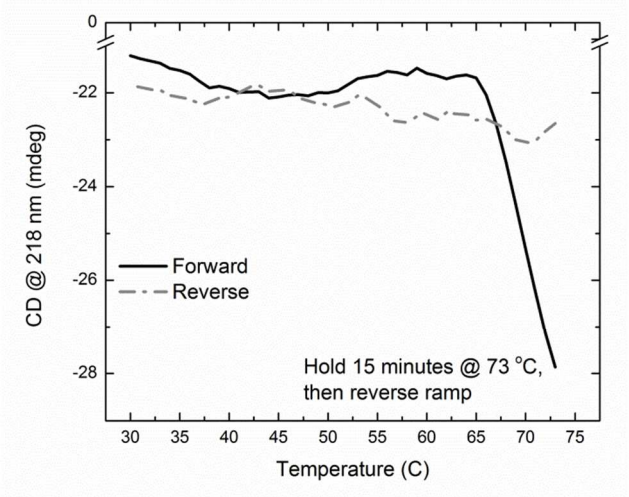

Figure S4: Forward then reverse temperature ramp in 500 mM trehalose. Both ramps were performed at a rate of 1 ^{0}C/min. The temperature was held at 73 ^{0}C (the maximum temperature of this ramp) for 15 minutes to evaluate the kinetic stability of the melting intermediate.

Figure S5 shows another forward and reverse temperature ramp, this time in mannitol. In this experiment we went beyond the intermediate by ramping the temperature up to 75 ^{0}C, and then cooled to determine if the protein unfolding up to that point was reversible. Fig. S5 shows that much, but not all of native signal was retained. From this experiment we can conclude that once the melt goes beyond the hump in the CD signal it is no longer reversible. Indeed, upon removal of the sample at 95 ^{0}C a white precipitate was observed in all conditions (but remained sufficiently well dispersed that the observed loss of CD signal could not be attributed to sedimentation, but to protein denaturation).

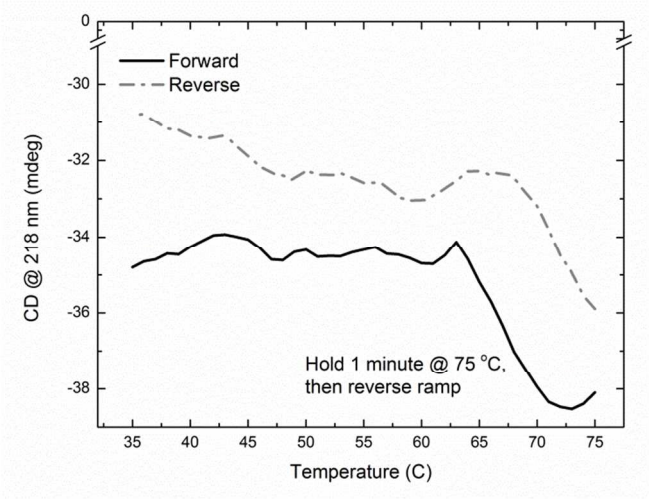

Figure S5: Forward and reverse temperature ramp in 500 mM Mannitol. Both ramp rates were 1 ^{0}C/min. The temperature was held at 75 ^{0}C for 1 minute before the reverse ramp initiated.

Normalization of CD Signals for Melts

The apparent melting temperatures reported in Table 1 of the article were determined by normalizing the CD signal to its maximum (*i.e.* the top of the hump); however, one may prefer to normalize by the native baseline. Figure S6 shows that the two normalization techniques yield results with near-perfect correlation.

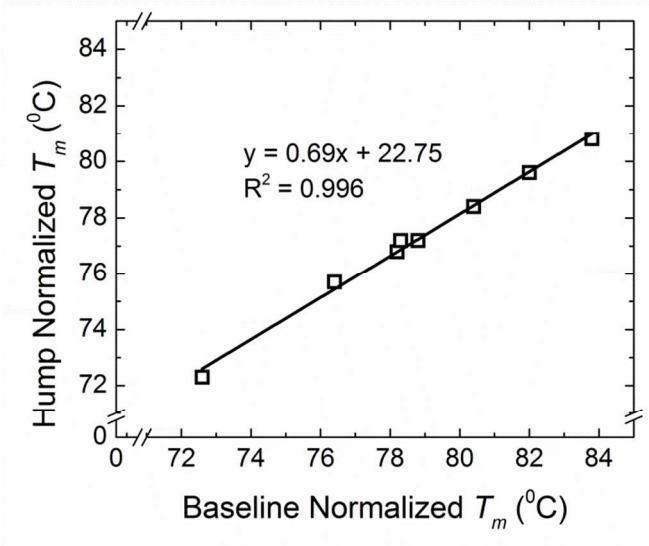

Figure S6: Correlation between T_m determined by baseline and hump normalization.

References:

1. Holthoff, H.; Schmitt, A.; Fernández-Barbero, A.; Borkovec, M.; Cabrerízo-Vílchez, M.A.; Schurtenberger, P.; Hidalgo-Alvarez, R., *J. Colloid Interface Sci.* **1997,** *192*,463-470.